SCIENCE CHINA
Information Sciences

• LETTER •

March 2026, Vol. 69, Iss. 3, 139401:1–139401:2
https://doi.org/10.1007/s11432-025-4494-2

High power density X-band source-connected field plate-free AlGaN/GaN HEMT with recessed gate oxidation process

Hao LU, Xiaohua MA*, Longge DENG, Ling YANG*, Bin HOU, Meng ZHANG, Mei WU & Yue HAO

School of Microelectronics, Xidian University, Xi'an 710071, China

Received 11 February 2025/Revised 21 April 2025/Accepted 11 June 2025/Published online 15 January 2026

Citation Lu H, Ma X H, Deng L G, et al. High power density X-band source-connected field plate-free AlGaN/GaN HEMT with recessed gate oxidation process. Sci China Inf Sci, 2026, 69(3): 139401, https://doi.org/10.1007/s11432-025-4494-2

GaN-based HEMTs have emerged as promising candidates for high-frequency and high-power RF applications owing to their superior intrinsic material properties [1]. Although source field plate (SFP) technology has been widely adopted to enhance power handling capability by mitigating peak electric fields at the gate-drain edge, it inevitably introduces undesirable effects such as increased Miller capacitance and process-induced performance fluctuations [2]. These limitations have motivated the development of alternative device architectures that can achieve comparable performance without employing SFP structures.

To address this issue, previous studies have demonstrated that the higher dielectric constant of AlGaN can effectively alleviate electric field concentration near the gate corner, consequently improving breakdown voltage [3]. This fundamental understanding has driven the advancement of recessed-gate designs aimed at redistributing the peak electric field from the SiN to the AlGaN interface. Nevertheless, conventional recessed-gate etching techniques frequently induce undesirable damage to the barrier layer, leading to elevated leakage currents and compromised device performance. In this work, we have implemented an oxide treatment process subsequent to the recessed gate etching. This critical post-processing step effectively repairs etching-induced defects, resulting in significant device performance enhancement. Our experimental results conclusively demonstrate the successful implementation of SFP-free AlGaN/GaN HEMTs for X-band applications, achieving excellent power density performance.

Experiment. Figure 1(a) illustrates the device structure schematic. Detailed information of the device structure and fabrication process can be found in Appendix A.

Results and discussion. Figure 1(b) reveals a smooth interface with 12 nm remaining AlGaN barrier thickness under the gate. Figure 1(c) presents the high-resolution transmission electron microscope (HRTEM) image of the oxide layer under the gate, showing a uniform 3-nm thick oxide layer formed through precise etching and optimized oxidation conditions. Figure 1(d) confirms the conformal coverage characteristics of the oxide layer during the plasma treatment process. Figures 1(e)–(h) demonstrate the continuous oxygen distribution at the gate metal/AlGaN interface through energy-dispersive X-ray spectroscopy (EDS) mapping. Combined with previously reported secondary ion mass spectrometry (SIMS) and X-ray photoelectron spectroscopy (XPS) results, the gate oxide layer is identified as a GaON/AlON composite [4]. Figures 1(i)–(l) further reveal through EDS mapping that the oxide formation extends to the etched SiN interface at gate corners.

As illustrated in Figure 1(m), the dual-sweep transfer I_{D}-V_{GS} characteristics of the two types of HEMTs are presented. For the RGO-HEMT, a high saturation drain current of 1.26 A/mm and a low leakage current of 4×10^{-7} A/mm are delivered, resulting in ON/OFF current ratio of over 10^6. The enhanced transconductance (g_{m}) of the RGO-HEMT results from the improved gate electrostatic control over the channel. Notably, the RGO-HEMT shows similar and negligible hysteresis in transfer I-V curves comparable to conventional HEMTs, confirming the high quality of the oxide interface. Figure 1(n) demonstrates that RGO-HEMTs achieve a 40 V higher breakdown voltage than conventional Schottky-gate HEMTs, resulting from effective electric field redistribution from the SiN/AlGaN interface to the AlON/GaON composite oxide layers. Significantly, the RGO-HEMT exhibits a breakdown voltage exceeding 200 V when measured at 10^{-2} A/mm current density. The overlapping I_{Gate} and I_{Drain} curves confirm gate-related leakage as the dominant breakdown mechanism. Figures 1(o) and (p) present pulsed I-V comparisons for both devices, revealing the superior dynamic performance of the RGO-HEMTs with only 10.1% current-collapse (CC) ratio at $(-8, 40)$ V bias conditions, markedly lower than conventional HEMTs (20.4%).

S-parameter small-signal characteristics have been measured for both devices. As shown in Figures 1(q) and (r), the peak $f_{\mathrm{T}}/f_{\mathrm{max}}$ of the RGO-HEMT are 46.2/63.0 GHz, while those for the conventional HEMTs are 41.1/54.5 GHz. These results show the proposed RGO-HEMT improved f_{max} and f_{T} while maintaining excellent breakdown characteristics. As shown in Figure 1(s), X-band load-pull measurements at 8 GHz (CW mode) demon-

* Corresponding author (email: xhma@xidian.edu.cn, yangling@xidian.edu.cn)

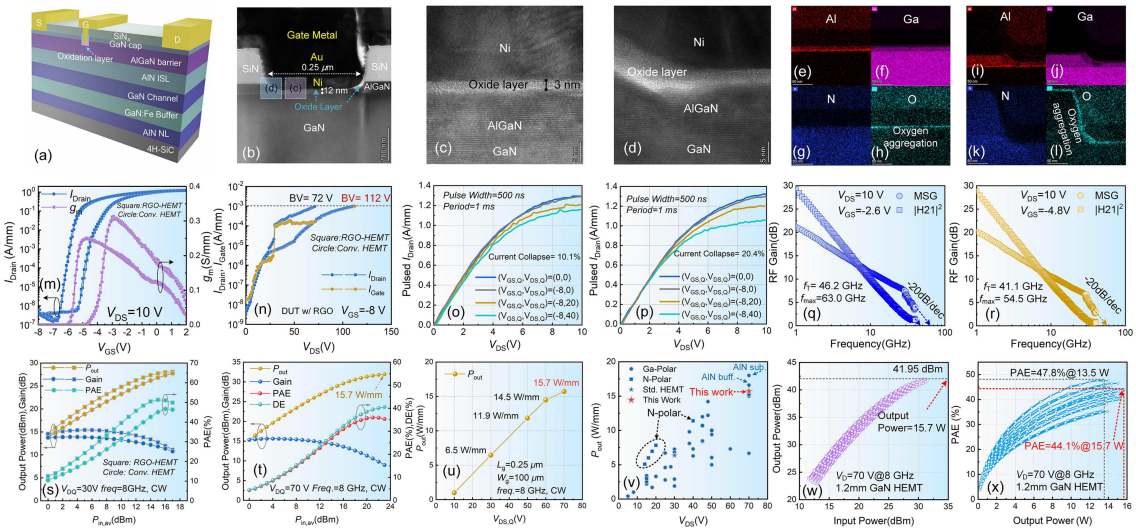

Figure 1 (Color online) (a) Schematic diagram and (b) cross-sectional micrograph view for the fabricated AlGaN/GaN HEMTs with the RGO process. HRTEM image of (c) the area beneath the gate and (d) the gate corner region. EDS mapping of the region under the gate metal: (e) Al, (f) Ga, (g) N, and (h) O elements. EDS mapping of the gate corner region: (i) Al, (j) Ga, (k) N, and (l) O elements. (m) Dual-sweep transfer *I*-*V* characteristics. (n) OFF-state breakdown characteristics. (o), (p) Pulsed *I*-*V* characteristics. (q), (r) RF small-signal characteristics comparison for both device types. (s) Large-signal power characteristics between the two types of HEMTs at $V_{\rm DS}$ = 30 V. (t) Large-signal power characteristics of RGO-HEMTs at $V_{\rm DS}$ = 70 V. (u) The $P_{\rm out}$ as a function of $V_{\rm DS}$ for the RGO-HEMTs. (v) X-band power performance benchmarking against literature data. (w) Output power and (x) PAE curves at multiple impedance points for the 1.2 mm RGO-HEMT at 70 V operation.

strate that the RGO-HEMTs achieved 51.3% peak PAE with 12.7 dB power gain at $V_{\rm DS}$ = 30 V, which shows a significant improvement over conventional HEMTs (46.7%, 11.3 dB). This enhancement stems from optimized transconductance and suppressed current collapse. Figure 1(t) reveals that the RGO-HEMTs delivered a high $P_{\rm out}$ of 15.7 W/mm while maintaining 15.2 dB linear gain at 70 V operation. Figure 1(u) displays that the RGO process maintains linearly increased $P_{\rm out}$ over a wide range of drain voltage variation. Figure 1(v) presents an X-band power performance benchmark comparison, demonstrating that the achieved results exceed the state-of-the-art performance reported for both Ga-polar and N-polar GaN HEMTs in existing literature. Future optimization will focus on novel termination and buffer design improvements [5]. A device with a large gate width of 1.2 mm was also fabricated using the air-bridge source connection technique. As shown in Figure 1(w), the device achieved 15.7 W (41.95 dBm) total output power at 70 V drain bias under pulsed operation (20 μs pulse width, 10% duty cycle), corresponding to 13.1 W/mm power density. Figure 1(x) depicts that the device achieves a PAE of 47.8% at an output power of 13.5 W and maintains 44.1% even at peak power. These results confirm the excellent power scaling capability of the RGO-HEMTs from 100-μm to 1.2-mm device geometries, validating their potential for practical high-power applications.

Conclusion. This study demonstrates high-performance AlGaN/GaN HEMTs on SiC substrates fabricated using a recessed gate oxidation process, achieving a power density of 15.7 W/mm at 70 V drain bias. The RGO-HEMTs exhibit excellent electrical characteristics including ultralow leakage current, negligible hysteresis, and minimal current collapse, validating the effectiveness of this approach for high-power RF applications. These results highlight the RGO technique in enhancing the power handling capacity of GaN-based devices.

Acknowledgements This work was supported by National Natural Science Foundation of China (Grant Nos. 62404165, 62474135, 62234009, 62090014), Natural Science Basic Research Program of Shaanxi (Grant No. 2024JC-YBQN-0611), China Postdoctoral Science Foundation (Grant Nos. 2023M732730, GZB20230557), and Fundamental Research Funds for the Central Universities of China (Grant Nos. ZYTS25217, QTZX25069, ZYTS25218).

Supporting information Appendix A. The supporting information is available online at info.scichina.com and link.springer.com. The supporting materials are published as submitted, without typesetting or editing. The responsibility for scientific accuracy and content remains entirely with the authors.

References

1 Zhang H, Wang H, Zhang M, et al. 2DEG-concentration-modulated high-power-density AlGaN/GaN RF HEMTs. IEEE Electron Device Lett, 2024, 45: 1157–1160
2 Wu Y F, Saxler A, Moore M, et al. 30-W/mm GaN HEMTs by field plate optimization. IEEE Electron Device Lett, 2004, 25: 117–119
3 Tahhan M B, Logan J A, Hardy M T, et al. Passivation schemes for ScAlN-barrier mm-Wave high electron mobility transistors. IEEE Trans Electron Device, 2022, 69: 962–967
4 Park J H, Hwang S K, Kim J, et al. N_2O plasma treatment effect on reliability of p-GaN gate AlGaN/GaN HEMTs. Appl Phys Lett, 2022, 120: 132103
5 Lu H, Hou B, Yang L, et al. High RF performance GaN-on-Si HEMTs with passivation implanted termination. IEEE Electron Device Lett, 2022, 43: 188–191